



PERGAMON

Continental Shelf Research 18 (1998) 677–693

CONTINENTAL SHELF
RESEARCH

Variation of residual current in Tokyo Bay due to increase of fresh water discharge

Xinyu Guo^{*,1}, Tetsuo Yanagi²

Department of Civil & Environmental Engineering, Ehime University, Matsuyama 790, Japan

Received 23 May 1996; accepted 9 December 1997

Abstract

Observed zooplankton data show that the number of outer bay species of zooplankton appearing in the central part of Tokyo Bay have increased in recent years. Because these zooplankton cannot reproduce in the inner bay, they must be brought into the bay by the advective transport of the sea water from the adjacent open ocean (Nomura, 1993 P. D. Thesis, Tokyo university of Fisheries). The increase of fresh water discharge is proposed as a mechanism for changing the residual current that is thought to bring the outer bay species of zooplankton into Tokyo Bay (Nomura, 1996, *Bulletin of Coastal Oceanography* 34, 25–35). To clarify the variation of the residual current due to the increase of fresh water discharge quantitatively, a three-dimensional prognostic numerical model is developed.

To verify of the prognostic numerical model, the observed temperature, salinity and residual current during the summer of 1979 are reproduced firstly. The calculated result confirms the existence of two eddies that have been reproduced by a diagnostic numerical model (Guo and Yanagi, 1996, *Journal of Oceanography* 52, 597–616). The first one is the anticlockwise circulation in the head region of the bay and the second one the clockwise circulation in the central part of the bay. Apart from these two eddies, the strong gravitational circulation at the mouth of the bay, which flows out of the bay in the upper layer and into the bay in the lower layer, is also reproduced. Next, the river discharge is increased to the level of the summer of 1989 and the calculation is carried out again. The difference between these two calculated results is considered as the variation induced by the increase of fresh water discharge.

The calculated result shows that the increase of river water influences the residual current in the head region of the bay greatly. At the mouth of the bay, the gravitational circulation is strengthened by up to 0.5 cm/s. This variation of residual current is expected to bring more

* Corresponding author.

¹ Present affiliation: Institute for Global Change Research, SEAVANS North 7F, 1-2-1 Shibaura, Minato-Ku, Tokyo 105, Japan.

² Present affiliation: Research Institute for Applied Mechanics, Kyushu University, 6-1 Kasuga-Kohen, Kasuga-city, Fukuoka 816, Japan.

outer bay species of zooplankton into the inner bay from the adjacent open ocean. © 1998 Elsevier Science Ltd. All rights reserved.

Keywords: Tokyo Bay; residual current; numerical model.

1. Introduction

Tokyo Bay is a semi-enclosed bay situated at the central part of Japan, which communicates with the Pacific Ocean through the narrow Uraga Strait (Fig.1). Being one of the most important bays in Japan, environmental changes at Tokyo Bay have been studied closely (Ogura, 1993).

Zooplankton data, collected in the central part of Tokyo Bay every month from 1981 to 1990, showed that the number of the outer bay species of zooplankton increased over the ten years, especially during the summer of each year (Nomura, 1993). It must be noted that in Nomura (1993), the outer bay species is defined as the zooplankton that cannot reproduce in the bay. Therefore they must be brought into the bay by the advective transport of the sea water from the mouth of the bay. Normally stratification in Tokyo Bay strengthens in spring and summer and weakens in autumn and winter. A northerly wind prevails over the bay in autumn, winter and spring, and a southerly wind dominates in summer (Unoki, *et al.*, 1980). These

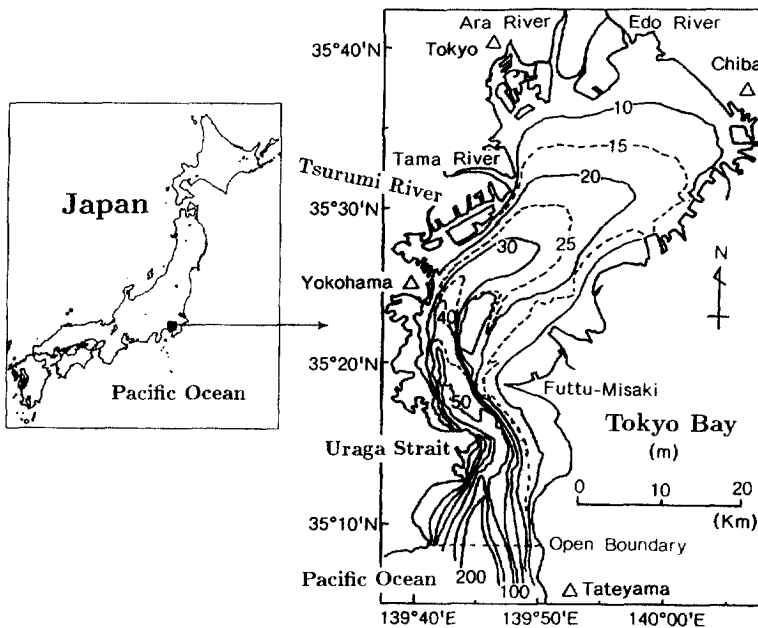


Fig. 1. Topography and rivers in Tokyo Bay. Numbers show the depth in meters and Δ 's denote the wind observation stations.

conditions induce a gravitational circulation at the mouth of the bay throughout the year, which flows out of the bay in the upper layer and into the bay in the lower layer (Unoki, 1985). If some changes in these conditions occurred over the ten years causing the gravitational circulation at the mouth of the bay to be enhanced, the outer bay species of zooplankton transported into the bay is likely to have increased.

Fig. 2 shows the annual variation of the wind velocity calculated from monthly mean wind speeds and prevailing wind directions and mean global solar radiation on August of each year from 1977 to 1993 at Stn. Tokyo (for the location of Stn. Tokyo, see Fig. 1). These data are drawn from the Annual Report of the Japan Meteorological Agency published by the Japan Meteorological Agency. There are no obvious overall trends. The same situation is found with the other months.

There are thirteen rivers that supply fresh water into the bay. The main four rivers are shown in Fig. 1. It is well known that the rivers around Tokyo Bay supply more than 90% of fresh water into the bay, and the precipitation and evaporation on the sea surface of the bay is nearly balanced in one year (Unoki, 1985). The discharges of the rivers are mainly controlled by dams that may reduce the seasonal variation of the fresh water discharge into the bay. Fig. 3 shows the annual averaged river discharge of Edo River, the largest river flowing into Tokyo Bay, from 1977 to 1993. Although the river discharge has a large variability, it appears to be increasing year to year. The population change from 1950 to 1992 around the bay, also shown in Fig. 3, shows a clear increase. Ogura (1993) showed that from 1936 to 1993 the population around Tokyo Bay increased about three times (from 0.9 to 2.6 billion). To meet the greater demand for fresh water from the increased population, water from some rivers which did not flow into Tokyo Bay before 1980s, has been drawn into the cities around the bay. This fresh water is therefore rerouted into Tokyo Bay. Because the observation station of the Edo River's discharge is located some distance from the entrance of the river into the bay, accurate data on this component of the fresh water discharge cannot be obtained now. However, considering that the monthly observed salinity in

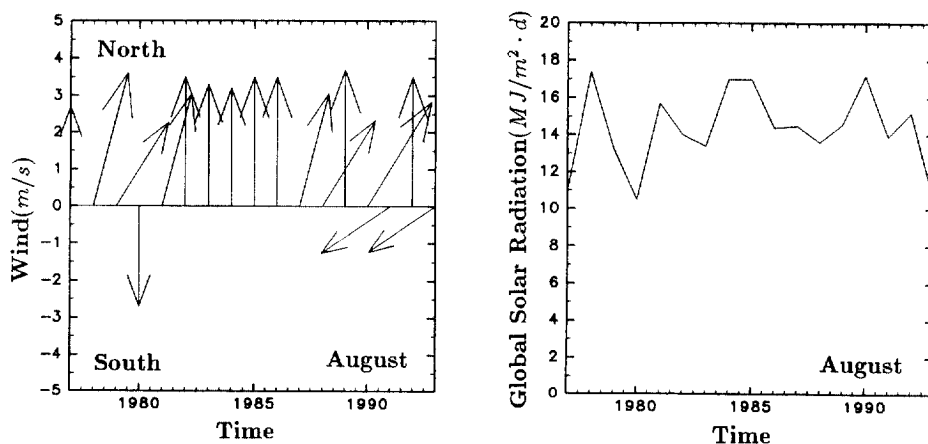


Fig. 2. The annual variation of monthly means of the wind and the global solar radiations at Stn. Tokyo.

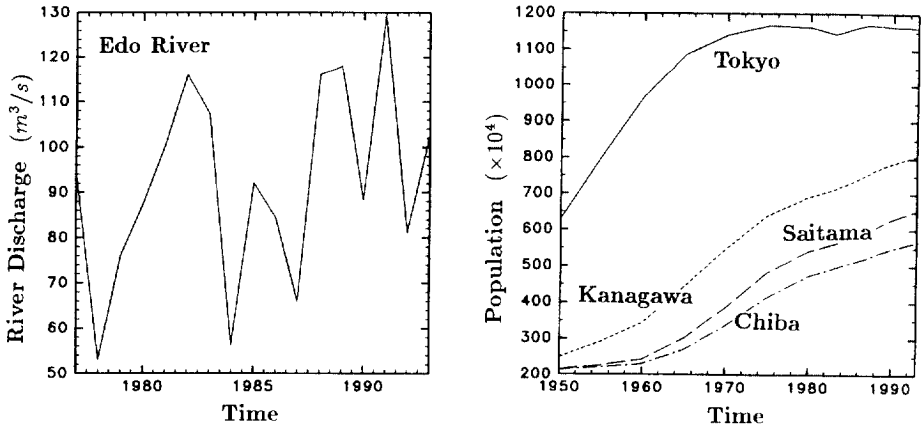


Fig. 3. The annual variation of the river discharge of Edo river and the annual variation of the population around Tokyo Bay.

the central part of the bay decreased from 1981 to 1990 (Nomura, 1996), it can be said that fresh water supply to Tokyo Bay has increased in recent years.

Although the fresh water discharge into Tokyo Bay has increased since the 1980's, how and to what extent this increased fresh water discharge influences the residual current system is not yet clear. To answer this question, a numerical model is needed.

There have been many studies on the residual current in Tokyo Bay, and a detailed review based on the observed data has been presented by Unoki (1985). Recently, Guo and Yanagi (1994, 1995, 1996) carried out a series of numerical experiments concerning the tidal current and the residual current in Tokyo Bay. The most recent experiment tried to clarify the seasonal variation of the residual current in Tokyo Bay by using a three-dimensional diagnostic numerical model. That study concluded that the seasonal variation of the residual current in Tokyo Bay can be attributed to the variation in the strength of two eddies. The first one is an anticlockwise circulation in the head region of the bay, which develops in spring and summer and disappears in autumn and winter. The second one is a clockwise circulation in the central part of the bay, which strengthens in autumn and winter, and diminishes in spring and summer (Guo and Yanagi, 1996). But as the temperature and salinity data used in this diagnostic calculation was obtained in 1979, the calculated residual current corresponds that of the bay in 1979.

In this paper, a three-dimensional prognostic numerical model is developed and used to investigate the influence of the increase in fresh water discharge on the residual current in Tokyo Bay during the summer. Special attention is paid to the verification of the numerical model by comparing its results with the observed data. By changing the boundary conditions in the numerical model, the influence of fresh water discharge change is studied and some quantitative conclusions are made.

2. Numerical Model

2.1. Formulation

The governing equations on the Cartesian (x, y, z) coordinate system, where the horizontal coordinate is laid out on the undisturbed sea surface and the vertical coordinate is directed upwards, are as follows:

$$\frac{\partial u}{\partial t} + \mathbf{u} \cdot \nabla u - fv = -\frac{1}{\rho_0} \frac{\partial P}{\partial x} + \frac{\partial}{\partial x} \left(A_h \frac{\partial u}{\partial x} \right) + \frac{\partial}{\partial y} \left(A_h \frac{\partial u}{\partial y} \right) + \frac{\partial}{\partial z} \left(A_v \frac{\partial u}{\partial z} \right) + T_x \tag{1}$$

$$\frac{\partial v}{\partial t} + \mathbf{u} \cdot \nabla v + fu = -\frac{1}{\rho_0} \frac{\partial P}{\partial y} + \frac{\partial}{\partial x} \left(A_h \frac{\partial v}{\partial x} \right) + \frac{\partial}{\partial y} \left(A_h \frac{\partial v}{\partial y} \right) + \frac{\partial}{\partial z} \left(A_v \frac{\partial v}{\partial z} \right) + T_y \tag{2}$$

$$P = \rho_0 g (\eta - z) + \rho_0 g \int_z^0 \frac{\rho - \rho_0}{\rho_0} dz' \tag{3}$$

$$\frac{\partial \eta}{\partial t} + \frac{\partial}{\partial x} \int_{-h}^0 u dz + \frac{\partial}{\partial y} \int_{-h}^0 v dz = 0 \tag{4}$$

$$\rho = F(T, S) \tag{5}$$

$$\frac{\partial T}{\partial t} + \mathbf{u} \cdot \nabla T = \frac{\partial}{\partial x} \left(K_h \frac{\partial T}{\partial x} \right) + \frac{\partial}{\partial y} \left(K_h \frac{\partial T}{\partial y} \right) + \frac{\partial}{\partial z} \left(K_v \frac{\partial T}{\partial z} \right) \tag{6}$$

$$\frac{\partial S}{\partial t} + \mathbf{u} \cdot \nabla S = \frac{\partial}{\partial x} \left(K_h \frac{\partial S}{\partial x} \right) + \frac{\partial}{\partial y} \left(K_h \frac{\partial S}{\partial y} \right) + \frac{\partial}{\partial z} \left(K_v \frac{\partial S}{\partial z} \right) \tag{7}$$

where

$$\mathbf{u} = u\mathbf{i} + v\mathbf{j} + w\mathbf{k}$$

$$\nabla = \mathbf{i} \frac{\partial}{\partial x} + \mathbf{j} \frac{\partial}{\partial y} + \mathbf{k} \frac{\partial}{\partial z}$$

t = time,

u, v, w = the x, y and z components of residual current,

P = pressure,

T = water temperature,

S = salinity,

ρ = density,

ρ_0 = reference density (the averaged value of all points),

h = undisturbed water depth,

η = sea surface elevation,

f = Coriolis parameter ($8.469 \times 10^{-5} \text{ s}^{-1}$),

g = acceleration due to gravity (980 cm/s^2).

T_x and T_y in equations (1) and (2) are tidal stresses and are defined as follows:

$$T_x = - \left\langle u_0 \frac{\partial u_0}{\partial x} + v_0 \frac{\partial u_0}{\partial y} + w_0 \frac{\partial u_0}{\partial z} \right\rangle \quad (8)$$

$$T_y = - \left\langle u_0 \frac{\partial v_0}{\partial x} + v_0 \frac{\partial v_0}{\partial y} + w_0 \frac{\partial v_0}{\partial z} \right\rangle \quad (9)$$

where, u_0, v_0, w_0 are the three components of the tidal current that have been calculated in advance (Guo and Yanagi, 1994) and $\langle \rangle$ denotes the tidal average. Equation (5) is the well-known Knudsen state equation.

The horizontal eddy viscosity (A_h) and diffusivity (K_h) are related to the amplitude of tidal current according to the tidal mixing theory:

$$A_h = \frac{\alpha}{2\pi} U_{amp}^2 T_{tide} \quad (10)$$

$$K_h = \frac{\beta}{2\pi} U_{amp}^2 T_{tide} \quad (11)$$

Here U_{amp} and T_{tide} are the amplitude and period of tidal current (M_2), respectively; α and β are the parameters used to adjust the horizontal eddy viscosity and diffusivity to a reasonable range. Considering that the amplitude of M_2 tidal current in Tokyo Bay varies over a range of 5–50 cm/s (Guo and Yanagi, 1994), the parameters α and β are set to 0.2 and 0.15, respectively. The resulting horizontal eddy viscosity and diffusivity are in the range of 1.0×10^5 – 1.0×10^7 cm^2/s . These values are similar to those found in other studies on the residual current in Tokyo Bay (Ikeda *et al.*, 1981; Yanagi and Shimizu, 1993) and have been used successfully in our diagnostic numerical calculations (Guo and Yanagi, 1996).

2.2. Turbulent closure model

It is well known that an incorrect formation of the vertical eddy viscosity (A_v) and diffusivity (K_v) is fatal to a prognostic numerical calculation in a stratified body of water (James, 1977; Sharples and Simpson, 1995). Observations in Tokyo Bay show a stratification existing in the bay throughout the year (Nomura, 1993). Thus a turbulent closure model that can include the effect of stratification is naturally preferred.

Following Sharples and Simpson (1995), we relate the vertical eddy viscosity and diffusivity to the local gradient Richardson number (R_i) by

$$A_v = S_M l q; \quad K_v = S_H l q. \quad (11)$$

Here S_M and S_H are stability functions that are ultimately dependent on R_i , via a flux Richardson number (R_f). A detailed expression for S_M and S_H can be found in Sharples and Simpson (1995).

The turbulent intensity, q , is calculated by assuming a local equilibrium between the shear and buoyancy productions of turbulent kinetic energy, and dissipation:

$$A_v \left[\left(\frac{\partial u}{\partial z} \right)^2 + \left(\frac{\partial v}{\partial z} \right)^2 \right] + K_v \left(\frac{g}{\rho_0} \frac{\partial \rho}{\partial z} \right) = \frac{q^3}{B_1 l} \quad (12)$$

The turbulent lengthscale l is chosen as:

$$l(z) = \kappa(z + h) \left(\frac{z}{h} \right)^{1/2} \quad (13)$$

where $\kappa = 0.41$ is von Karman's constant.

As pointed out by Sharples and Simpson (1995), this scheme has the weakness of causing all vertical transport above a critical gradient Richardson number to go to zero. In this case the critical number is $R_i = 1/3$. Because this condition of zero vertical transport is physically unrealistic, they suggested that a background viscosity, below which A_v and K_v are not allowed to fall, could be introduced to overcome this weakness. Such method can also be found in other studies (James, 1977; Takeoka *et al.*, 1991) and is adopted in our model.

However, when we incorporated the above scheme into our numerical model, we found that the Richardson number is difficult to estimate with high precision. When the water in the upper layer is heavier than that in the lower layer, the numerical model will immediately overturn the water. Therefore the Richardson number cannot be negative in the calculation. This means that the above turbulent closure model may take effect only in a very narrow range ($0 \leq R_i \leq 1/3$). In other words, a bad estimation of the Richardson number may induce the above scheme to lose its advantage.

The precision of Richardson number in our numerical model is mainly determined by two factors. The first one is how to include the vertical shear due to a tidal current that has not been calculated at the same time as the residual current. James (1977) calculated the vertical shears due to the tidal current by assuming the logarithmic law for the vertical distribution of the tidal current above the sea bottom and added this vertical shear to the shear due to the residual current. In our calculation, we keep the idea of combining these two vertical shears linearly but we estimate the vertical shear due to the tidal current directly from the calculated three dimensional M_2 tidal current field (Guo and Yanagi, 1994) by:

$$U_T^2 = \left\langle \left(\frac{\partial u_0}{\partial z} \right)^2 + \left(\frac{\partial v_0}{\partial z} \right)^2 \right\rangle \quad (15)$$

Compared to the method used by James (1977) which just includes the information of bottom frictional stress due to the tidal current, equation (15) is expected to give a more accurate solution for the vertical shear.

The second factor is the resolution ability of numerical model in the vertical direction. The vertical distribution of a scalar quantity such as water temperature and salinity is generally monotonic, but velocity is more complicated. Thus if the number of mesh points in the vertical direction is not enough to represent the distribution of

the current, the calculated Richardson number may be larger than that in the real sea. This error will cause the numerical model to tend to assign the background values to the vertical eddy viscosity and diffusivity coefficient. Considering the capacity of our computer, we chose to divide the water column vertically into ten layers equidistant at each horizontal mesh point. This choice is considered to be adequate for correctly representing the vertical distribution of flow (Guo and Yanagi, 1996). In fact, a test run of the numerical model with twenty layers showed a very similar result to the model with ten layers. Finally, the Richardson number is calculated by

$$R_i = -\frac{g}{\rho_0} \frac{\partial \rho}{\partial z} \left/ \left[\left(\frac{\partial u}{\partial z} \right)^2 + \left(\frac{\partial v}{\partial z} \right)^2 + U_T^2 \right] \right. \quad (16)$$

2.3. Application to Tokyo Bay

The topography of Tokyo Bay is shown in Fig. 1. The maximum depth in this calculation is taken as 200 m for the computational economy. The horizontal grid size is 1 km × 1 km. The time step is 36 s.

The boundary conditions of the momentum flux through the sea surface and bottom are:

$$z = 0: \quad A_v \frac{\partial}{\partial z} (u, v) = \frac{1}{\rho_0} (\tau_x^a, \tau_y^a) \quad (17)$$

$$z = -h: \quad A_v \frac{\partial}{\partial z} (u, v) = \frac{1}{\rho_0} (\tau_x^b, \tau_y^b) \quad (18)$$

where the wind stresses τ_x^a, τ_y^a and sea bed stresses τ_x^b, τ_y^b are calculated as:

$$(\tau_x^a, \tau_y^a) = \rho_a C_d (u_a, v_a) \sqrt{u_a^2 + v_a^2} \quad (19)$$

$$(\tau_x^b, \tau_y^b) = \rho C_b (u_b, v_b) \sqrt{u_b^2 + v_b^2} \quad (20)$$

The symbols u_a and v_a denote the eastward and northward components of the wind velocity, $\rho_a (= 1.2 \times 10^{-3} \text{ g/cm}^3)$ is the density of air, $C_d (= 1.3 \times 10^{-3})$ is the non-dimensional drag coefficient at the surface, u_b and v_b are the velocities above the sea bed, and $C_b (= 2.6 \times 10^{-3})$ is the drag coefficient at the sea bed.

The boundary conditions of the heat flux through the sea surface and bottom are:

$$z = 0: \quad K_v \frac{\partial T}{\partial z} = \frac{Q_s}{\rho_0 C_p} \quad (21)$$

$$z = -h: \quad K_v \frac{\partial T}{\partial z} = 0. \quad (22)$$

where Q_s is the heat flux through the sea surface, and C_p is the specific heat under constant pressure.

The fluxes of salinity through the sea surface and bottom are assumed to be zero. As a result, the decrease of salinity in the bay is completely controlled by the inflow of

fresh water from the rivers. This efflux of salinity is expressed as:

$$K_h \frac{\partial S}{\partial n} dn H_R = Q_R \times (S_R - S) \quad (23)$$

where Q_R denotes the river discharge, S_R the salinity of river water, n the direction normal to the horizontal boundary and H_R the influenced depth of river water.

The non-slip condition for velocity and the no flux condition for heat and salinity are given along the coastal line except at the mesh points coinciding with each river mouth where equation (23) is applied. For the open boundary, a sponge condition of velocity is applied along six grids lines from the south boundary, and the observed temperature and salinity are kept constant there.

The numerical solving method for above equations is nearly the same as that used in the diagnostic numerical calculations (Guo and Yanagi, 1996). Referring to Ohnishi (1978), the transport equations of water temperature and salinity are solved numerically. Initially, a state of rest is assumed and an initial temperature and salinity field are given. The initial value of water temperature is set at 19°C (0–5 m), 18°C (5–20 m), 17°C (20–50 m) and 16°C (50–200 m). The initial value of salinity is set to decrease linearly from the head of the bay (29 psu) to the mouth of the bay (32 psu) in the upper layer (0–10 m) in order to cut down on calculation time. Below 10 m, a constant salinity of 34.5 psu is given at all mesh points. The calculation is run for fourteen days at which point the kinetic energy of the whole sea region reaches a steady state.

3. Results

3.1. CASE79

At first, we attempted to reproduce the observed water temperature, salinity and residual current in the summer of 1979 (Unoki *et al.*, 1980). Following Yanagi and Shimizu (1993), the heat flux through the sea surface (Q_s) is given as 150 W/m². The river discharges of Edo River, Ara River, Tama River and Tsurumi River (Fig. 1) in the summer are drawn from the 1979 Annual Report on River Discharge in Japan published by River Bureau, Ministry of Construction, Japan. The values used are 70, 30, 20 and 10 m³/s, respectively. The wind data collected during the observation period at four stations around Tokyo Bay (Tokyo, Chiba, Yokohama and Tateyama, shown by the triangles in Fig. 1) are averaged and interpolated to the calculated meshes. The results show that a southwest wind of about 5 m/s prevailed over Tokyo Bay during the observation period.

The calculated water temperature, salinity and density at two depths in the summer of 1979 are shown in Fig. 4, and the observed distribution at the same depth are shown in Fig. 5. The main characteristics in the observed distribution such as the cold water near the western coast and the salinity front in the central part of the bay are reproduced well by the model. For an easy comparison, the calculated and observed water temperature, salinity and density at the observation points are plotted against each other in Fig. 6. It is clear that salinity is not reproduced as well as water

CASE79

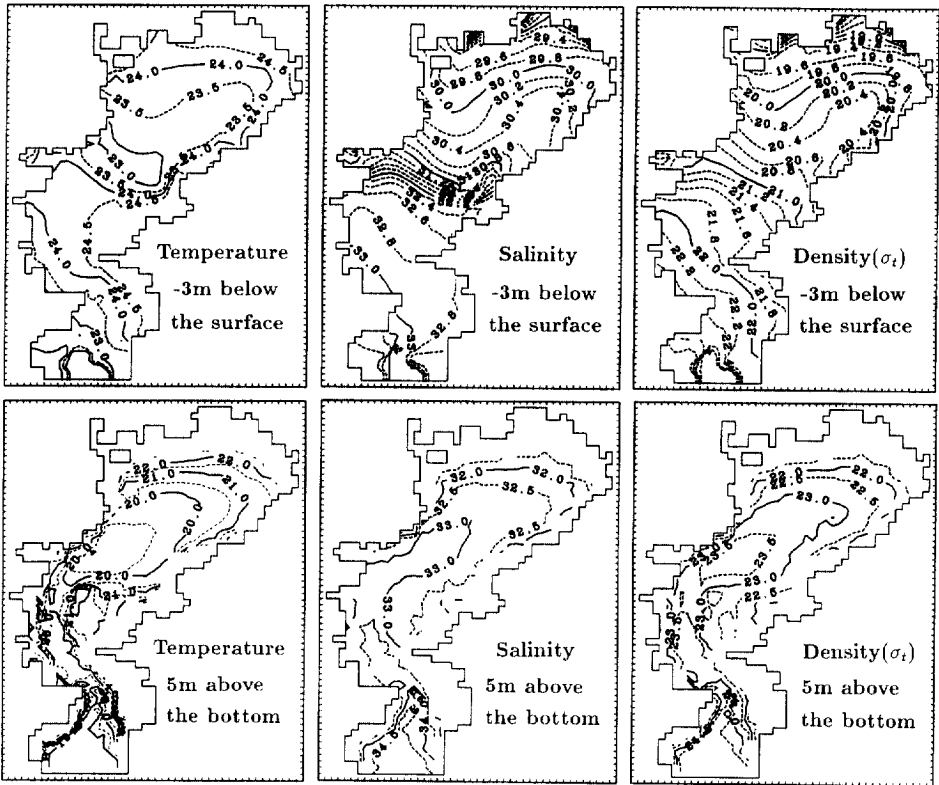


Fig. 4. Calculated water temperature, salinity and density in CASE79.

temperature. However, overall the calculation may be thought to reproduce the observed water temperature, salinity and density well.

The calculated and observed residual currents are shown in Fig. 7. In the upper layer, the calculated results show two eddies existing in the head region and the central part of the bay, which are also suggested by the observed current measurements. Quantitatively, the clockwise eddy in the central part of the bay calculated by the model is nearly the same as the observed eddy, but the calculated anticlockwise eddy in the head region is larger than the observations shown. In the lower layer, the calculated results coincide well with the observed pattern. At the mouth of the bay, the area that we want to know in the most detail, the obvious gravitational circulation in the observations is reproduced well by the model, both qualitatively and quantitatively.

For a deeper insight into the three-dimensional structure of the residual current in Tokyo Bay, the distribution of the residual current across four sections are shown in Fig. 8. At the mouth of the bay (section 1), a gravitational circulation of about 5 cm/s, with maximum speeds of 10 cm/s develops. In the central part of the bay

OBSERVATION

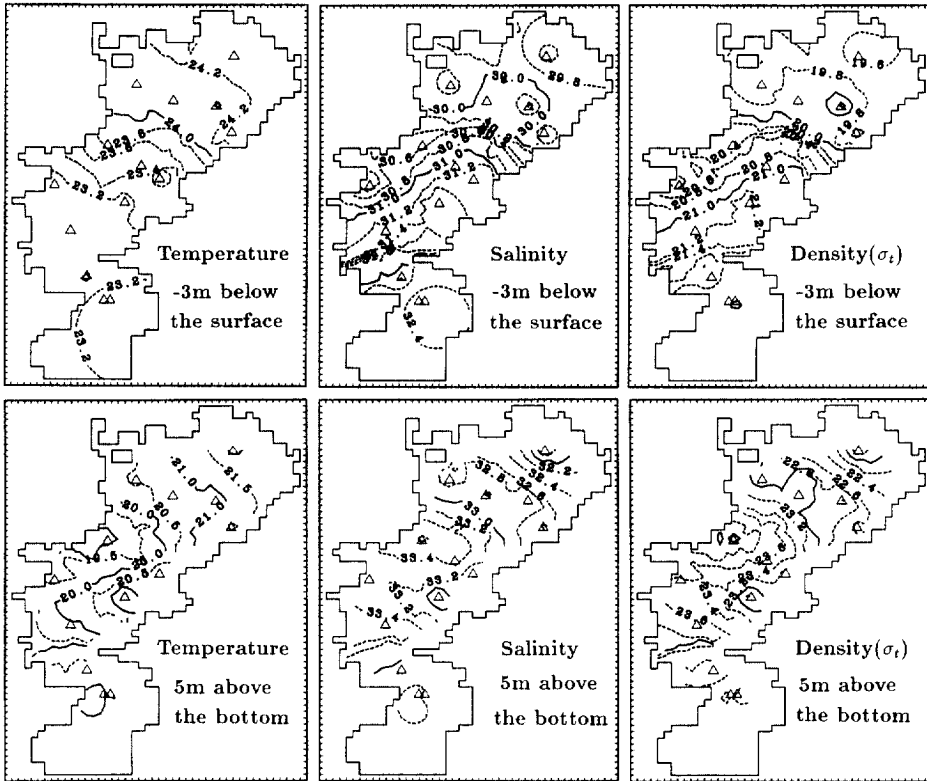


Fig. 5. Observed water temperature, salinity and density in the summer of 1979. The triangles show the observed points.

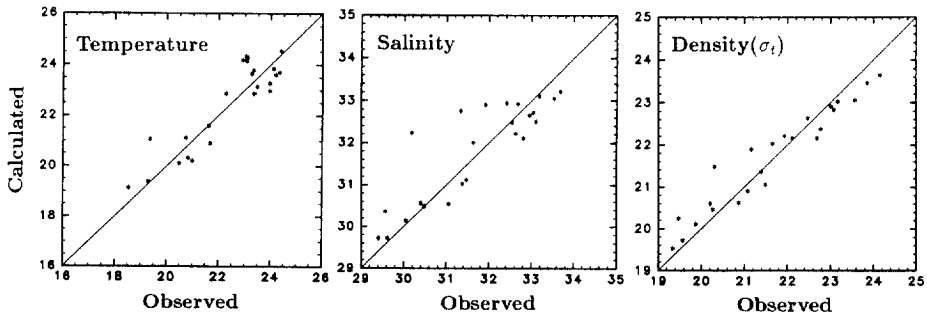


Fig. 6. Comparison of observed and calculated water temperature, salinity and density at the observed points.

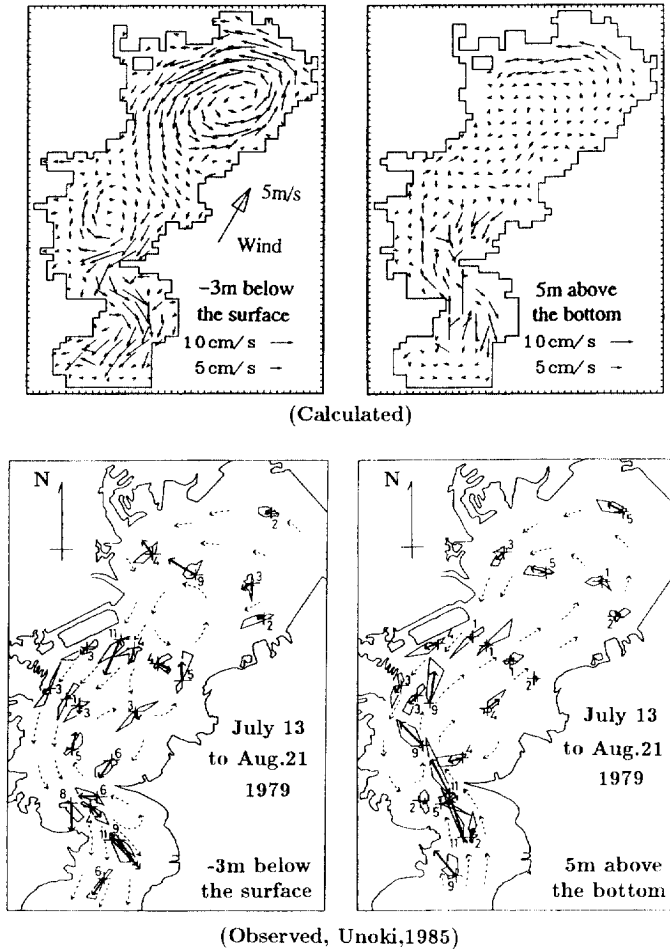


Fig. 7. Calculated and observed residual currents in the summer of 1979. The dotted lines in the observed results are the estimated flow pattern and the numbers show the speed of the flow in cm/s (Unoki, 1985).

(section 2), the clockwise circulation can be found at all depths. In the head region of the bay (sections 3 and 4), the anticlockwise circulation exists throughout the water column.

3.2. CASE89

Next, we used the numerical model to calculate the currents in the summer of 1989. The only changes are that the river discharges are increased to the level of the summer of 1989. The new river discharges of Edo River, Ara River, Tama River and Tsurumi River are 200, 70, 40 and 15 m³/s, respectively. The calculated water temperature, salinity and density distributions are shown in Fig. 9.

CASE79

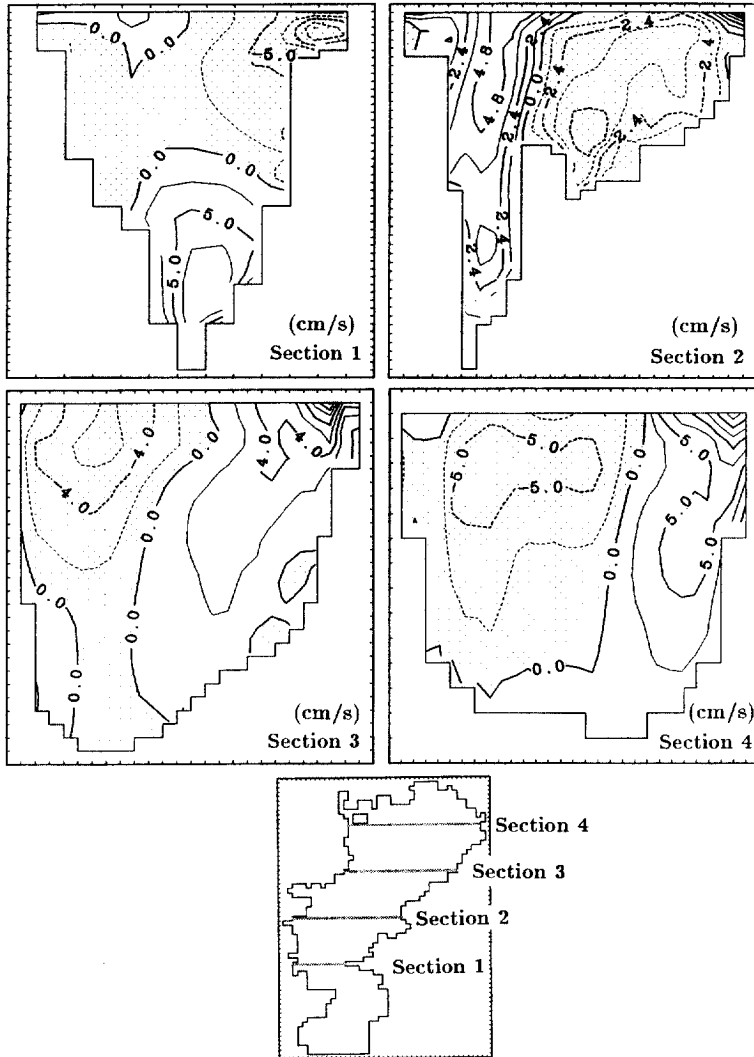


Fig. 8. Distribution of the residual current through four sections. Positive values show northward currents and negative values southward currents.

As expected, the water temperature varied little from the 1979 case but the salinity in the head region of the bay decreased greatly. Because this decrease does not change the basic pattern of salinity distribution, the calculated residual current is very similar to that calculated for 1979. The difference between these two cases will be discussed next.

CASE89

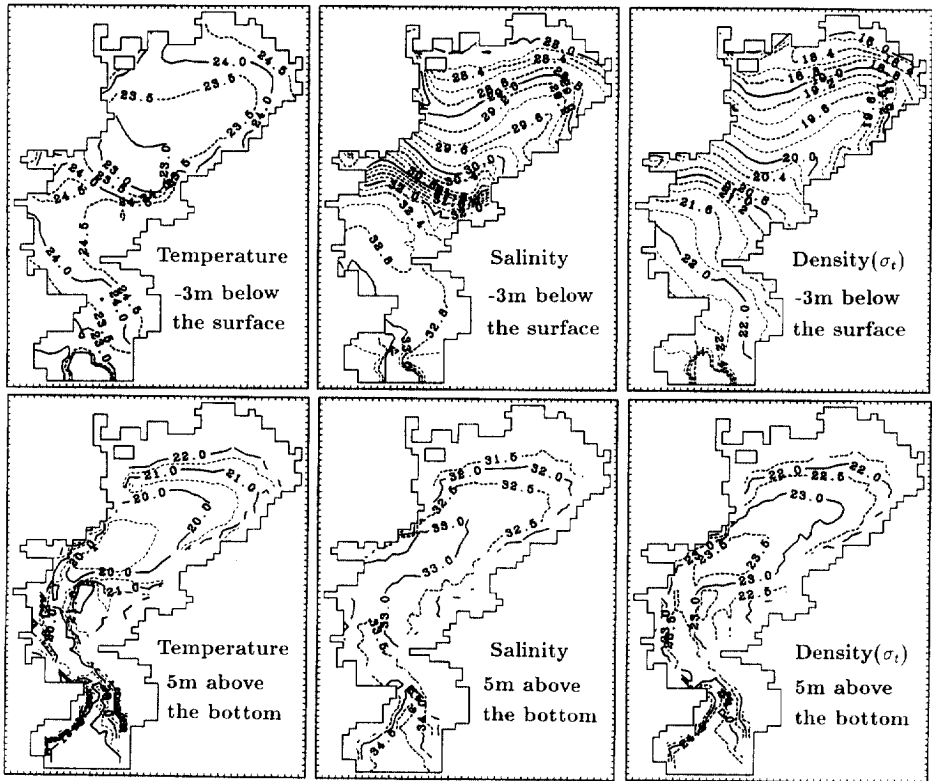


Fig. 9. Calculated water temperature, salinity and density in CASE89.

DIFFERENCE

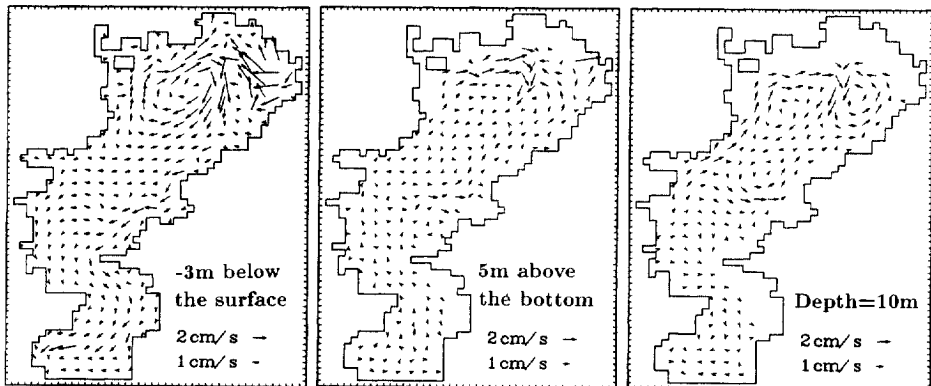


Fig. 10. Difference of the residual current between CASE79 and CASE89.

3.3. The variation of residual current

Fig. 10 shows the difference between the residual currents for CASE79 and CASE89 (CASE89-CASE79) at three depths. The influence of the increase in fresh water discharge on the residual current is strongest in the head region of the bay where the anticlockwise circulation seems to be decreased. In other places, such as the central part and the mouth of the bay, the variation is smaller, but the difference in residual current appears to flow out of the bay in the upper layer and into that bay in the lower layer.

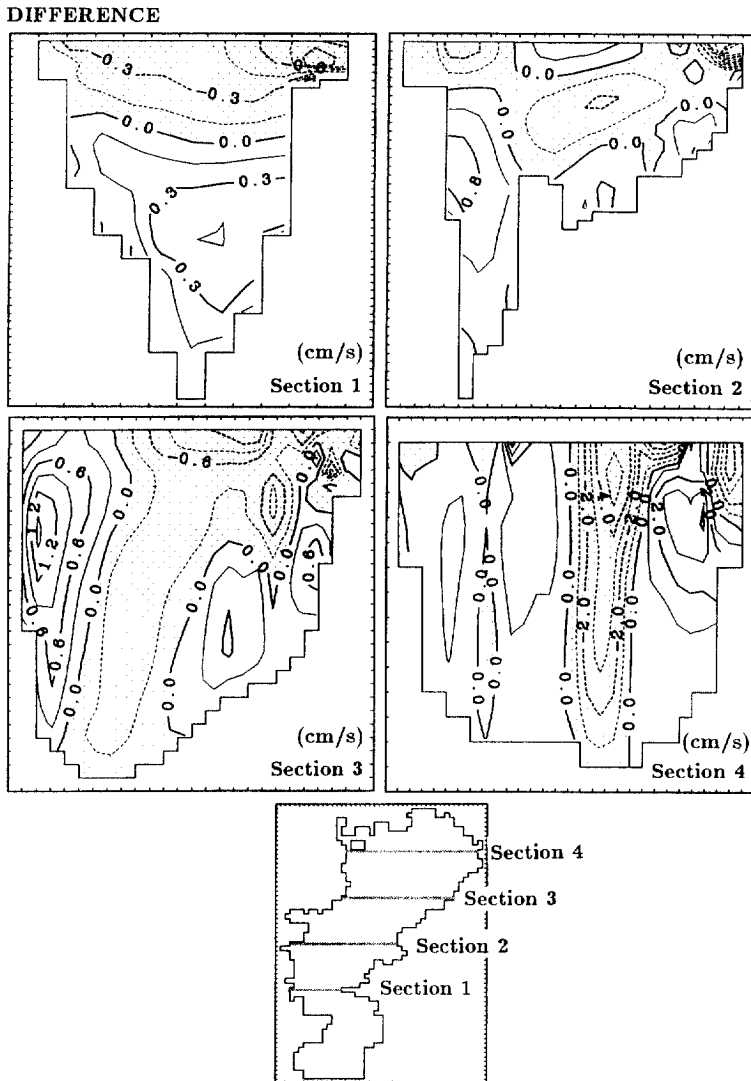


Fig. 11. Difference of the residual current between CASE79 and CASE89 through four sections. Positive values show northward currents and negative values southward currents.

The above difference between the residual currents for the two cases are shown across four sections in Fig. 11. It is interesting that the form of the residual current difference is very different in each section. In the head region, the residual current difference forms two eddies from the sea surface to the bottom. But at the mouth of the bay, the residual current difference forms a gravitational circulation. For more discussions about the reason of these difference, more numerical experiments is needed. Here what we are concerned about is the variation of the residual current at the mouth of the bay. This variation should be responsible for the increase of the number of outer bay species of zooplankton in the central part of the bay. Our calculations show that the gravitational circulation at the mouth of the bay is enhanced by up to 0.5 cm/s by the increase of the fresh water discharge as shown in Fig. 11.

4. Discussion

There are some problems in this study. The first one is the flux type boundary condition (equation (23)) which does not consider the inflow of fresh water itself. This omission is expected to have little influence on the residual current itself because the river discharge is relatively small compared to the volume of the bay. But the influence on the variation of residual current, may be larger. Because we do not have detailed residual current data at the mouth of the bay, we have no method to evaluate correctly the river discharge in our model now. In the future, we will try to clarify this influence.

The second problem is the open boundary condition used in this model. The values of water temperature and salinity are assumed to be the same in the two cases, but it is possible that some variations have occurred in the real sea. However, what we want to know is the effect of the increase of fresh water discharge on the residual current. In fact, the calculated residual current in CASE89 is not the real residual current in the summer of 1989 because the surface heat flux and the wind condition used in CASE89 is the same as that used in CASE79. On the other hand, sensitivity analyses show that small changes in the water temperature and salinity along the open boundary have little influence on the residual current in the inner part of the bay. This means that the variation of the residual current at the mouth of the bay is induced mainly by the variations in the inner part of the bay.

The distance from section 1 to the open boundary is 20 km and therefore may be not far enough for the calculated results at that section to be reliable. But the comparison with the observed data (Fig. 7) shows that the calculation is good enough to reproduce the gravitational circulation at the mouth of the bay. In addition, the strong mixing at the mouth of bay may reduce the effect from the open boundary greatly.

Increases of population around coastal seas can be found in many areas all over the world. Usually the influence of this population increase on the ecosystem in the coastal water is thought to be caused mainly by the increase of pollutant or nutrient loading. But it should be emphasized that variations of the residual current in the coastal water cannot be ignored because the residual current plays an important role

in the ecosystem. In particular, we emphasize the variations in the residual current at the boundary of the coastal water and the open ocean, that can change the structure of the ecosystem in the coastal region.

Acknowledgements

The authors are grateful to Drs. H. Takeoka, Y. Isoda and H. Nomura for their helpful suggestions about the results presented in this paper. We thank Drs. H. Akiyama and S. Takahashi for their useful discussions during the study. Thanks are also given to Mr. Steven Kraines who helped us to correct the English errors of this paper. The calculation was carried out on the workstation of Department of Civil & Environmental Engineering, Ehime University, and the 'DENNOU' graphic library was used to draw the figures. This study is partly supported by the research fund defrayed from the Ministry of Education, Science, Culture and Sports, Japan.

References

- Guo, X., Yanagi, T. 1994. Three dimensional structure of tidal currents in Tokyo Bay, Japan. *La mer* 32, 173–185.
- Guo, X., Yanagi, T. 1995. Wind-driven current in Tokyo Bay, Japan during winter. *La mer* 33, 51–64.
- Guo, X., Yanagi, T. 1996. Seasonal variation of residual current in Tokyo Bay, Japan – Diagnostic numerical experiments. *Journal of Oceanography* 52, 597–616.
- Ikeda, K., Matsuyama, M., Tsuji, M. 1981. Effect of the wind on the current in Tokyo Bay. *Umi to Sora* 57(1), 31–40 (In Japanese with English abstract and captions).
- James, I. D. 1977. A model of the annual cycle of temperature in a frontal region of the Celtic Sea. *Estuarine and Coastal Marine Science* 5, 339–353.
- Nomura, H. 1993. The species structure and transport process of zooplankton in Tokyo Bay. Ph.D. Thesis, Tokyo University of Fisheries (in Japanese).
- Nomura, H. 1995. Long-term variations of environmental parameters in Tokyo Bay, central Japan. *La mer*, 33, 107–118 (in Japanese with English abstract and captions).
- Nomura, H. 1996. Interaction between the inlet and the open ocean: A biological approach using time-series record of meso- and macrozooplankton community structure in Tokyo Bay. *Bulletin of Coastal Oceanography* 34, 25–35 (In Japanese with English abstract and captions).
- Ogura, N. (ed.), 1993. Tokyo Bay – Its Environmental Changes. Koseisha Koseikaku, Tokyo (in Japanese).
- Oonishi, Y. 1978. The numerical research – its methods. In Horibe (ed.), *Oceanography as an Environmental Science*, vol.2, Tokyo University Press, Tokyo, pp. 246–271 (in Japanese).
- Sharples, J., Simpson, J.H. 1995. Semi-diurnal and longer period stability cycles in the Liverpool Bay region of freshwater influence. *Continental Shelf Research* 15, 295–313.
- Takeoka, H., Ohno, Y., Inahata, N. 1991. Roles of horizontal processes in the formation of density stratification in Hiuchi-Nada. *Journal of the Oceanographical Society of Japan* 47, 33–44.
- Unoki, S., Okazaki, M., Nagashima, H. 1980. The circulation and oceanic condition in Tokyo Bay. Report of Physical Oceanography Laboratory in Physical-Chemical Institute, No.4, (in Japanese).
- Unoki, S. 1985. Tokyo Bay-its physical aspect. In *Coastal Oceanography of Japanese Islands*. Tokai University Press, Tokyo, pp. 341–361 (in Japanese).
- Yanagi, T. 1989. Coastal Oceanography. Koseisha-Koseikaku, Tokyo (in Japanese).
- Yanagi, T., Shimizu, M. 1993. Sedimentation processes in Tokyo Bay, Japan. *La mer* 31, 91–101.